PHYSICAL REVIEW B **79**, 121309(R) (2009)

Spatially resolved low-frequency noise measured by atomic force microscopy

Lynda Cockins, Yoichi Miyahara,* and Peter Grutter
Department of Physics, McGill University, 3600 rue University, Montreal, Canada H3A 2T8

(Received 23 January 2009; revised manuscript received 26 February 2009; published 31 March 2009)

We report spatially resolved charge noise measurements on semiconductor samples by atomic force microscopy. We observed charge noise induced by light illumination on an InP/InGaAs heterostructure with surface InAs quantum dots and a buried two-dimensional electron gas. The observed noise exhibits generation-recombination noise or random telegraph noise depending on light intensity and bias voltage. A spatial resolution better than 20 nm was demonstrated by comparing the noise on and off the InAs quantum dots. The approach enables the localization of individual traps and will aid in understanding noise mechanisms.

DOI: 10.1103/PhysRevB.79.121309 PACS number(s): 68.37.Ps, 72.40.+w, 78.67.−n, 73.22.−f

A detailed understanding of electrical noise is essential for improving the performance and reliability of semiconductor devices. Particularly detrimental, especially when using small volumes, are types of noise that arise due to localized energy states which act as charge traps. Noise arising from trapping and detrapping of charge, known as generation-recombination (G-R) noise,[1] has been of fundamental importance in developing electrical devices.[2,3] G-R noise has a Lorentzian frequency spectrum with increasing amplitude at lower frequency, thus having greater effect on low-frequency performance. Nanometer scale devices containing a single or few traps often exhibit random telegraph noise (RTN), a form of G-R noise, which can drastically affect the operation of such small devices. G-R noise can be used to study the properties of charge traps.[2] However conventional noise measurements are performed by electric transport measurements which give only spatially averaged information from various trapped charges and very limited information about the location of each trap even if a single trap is involved.

Scanning tunneling microscopy has been used for spatially mapping charge trapping events.[4–7] However, this technique is limited to traps located near noninsulating surfaces because a tunneling current of at least several picoamperes is typically required. Another way of measuring low-frequency noise is with sensitive electrometers which detect the fluctuation in electrostatic potential associated with charge trapping/detrapping events.[8,9] Noise measurements using such electrometers were performed using a single-electron transistor[10,11] or quantum point contact[12,13] placed nearby the device under test. A scanning electrometer based on the integer quantum Hall effect was devised and applied to local noise-voltage mapping.[14,15]

It is known that electrostatic force detection by atomic force microscopy (AFM) can also be used as an electrometer with single-electron sensitivity.[16–18] The long-range nature of the electrostatic force enables the detection of charge traps residing not only on the sample surface but also in the bulk.[19] This method does not require a current passed through the sample, simplifying noise interpretation as conducting leads often contribute to electrical noise.

By using electrostatic force detection with AFM, called electrostatic force microscopy (EFM), we observed local charge noise induced by light illumination on an InP/InGaAs heterostructure with surface InAs quantum dots (QDs) and a buried two-dimensional electron gas. We studied self-assembled InAs QDs on InP grown by chemical beam epitaxy.[20] The structure consists of 460 nm undoped InP grown on top of an InP substrate, followed by a 10 nm Si-doped InP layer, 10 nm undoped layer, 20 nm $In_{0.53}Ga_{0.47}As$ layer, 20 nm undoped layer, and finally a 1.82 ML InAs layer which forms the InAs QDs. The typical base diameter and height of the QDs are 50 and 10 nm, respectively. Electrical contact to the sample was made to the two-dimensional electron gas formed in the $In_{0.53}Ga_{0.47}As$ layer (20 nm below the surface) by indium diffusion. All reported dc bias voltages V_s were applied to this back electrode with respect to the grounded cantilever.

The experiments were performed with our homebuilt 4 K AFM.[21] Commercially available Si AFM cantilevers[22] were sputter coated with a 10 nm Ti layer followed by 20 nm Pt layer to ensure good electrical conduction and to exclude any photoinduced effects in the tip. The radius of the coated tip was approximately 10–15 nm. The coated cantilevers typically show a quality factor of ~100 000 and ~30 000, in vacuum (1×10^{-4} mbar), at 4.5 and 77 K, respectively. The AFM is equipped with two optical fibers. The first (1550 nm light) detects cantilever deflection with a fiber-optic interferometer,[23] while the second (780 nm light) is directed toward the sample surface with a maximum intensity of ~150 nW/mm^2. The 780 nm light has energy larger than the band gaps of InAs and InP. The AFM was operated in frequency modulation (FM) mode.[24] The experiments were performed at 4.5 and 77 K.

Figure 1 shows topographic images with the illumination (a) off and (b) on. We refer to these images as "EFM topography" because each line scan represents a profile of constant electrostatic force (constant Δf) induced by an applied dc bias V_s. Imaging the surface while the laser was on showed many streaks, in the fast scan direction, that were not present when the laser was off. The streaks mostly disappear in the images where the applied sample bias voltage V_s cancels the tip-sample contact potential difference (CPD) thereby minimizing the electrostatic force; this indicates that the streaks are due to noise in the electrostatic force.

After positioning the cantilever tip over one location, the time trace of the resonance frequency shift Δf was acquired for 10 s (with 1 kHz sampling rate) at a constant tip height

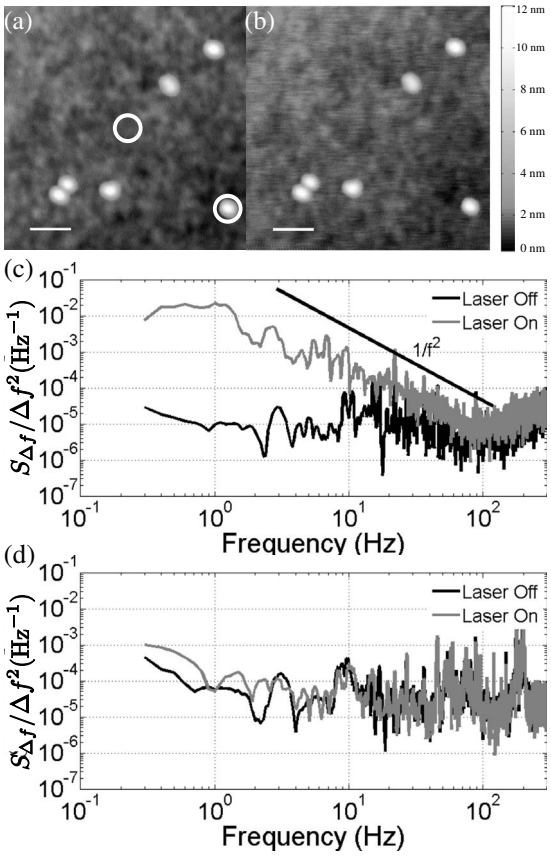

FIG. 1. EFM topography images taken with laser (a) off and (b) on. Both images were taken in constant frequency shift mode (Δf =−31.66 Hz) with V_s=2 V at 4.5 K. Scale bars=200 nm. The EFM image with the laser on (b) shows noise (streaks) along the fast scan (horizontal) direction. This noise is characterized by measuring Δf over the wetting layer [center circle in (a)] and the quantum dot [lower circle in (a)] at a constant height for 10 s. The PSD spectra ($S_{\Delta f}/\Delta f^2$) of the Δf shows increased low-frequency (<100 Hz) noise with laser irradiation only (c) over the wetting layer and not (d) over the quantum dot. This noise follows a $1/f^2$ dependence which indicates generation-recombination noise.

with laser off and on, at different V_s, and laser intensities, over the wetting layer (WL) and over the QD. The power spectral density (PSD) of the acquired Δf taken over the WL and over an InAs QD for a V_s=2 V are shown in Figs. 1(c) and 1(d), respectively.[25] Over the WL, a clear increase in low-frequency noise is observed upon laser irradiation. This noise follows a $1/f^2$ dependence which agrees with a Lorentzian spectrum indicating G-R noise.[3] The PSD spectra over the QD, however, show no change upon laser irradiation for all applied laser intensities and V_s despite the smaller band gap of InAs compared to InP.

We can estimate the spatial resolution of this technique by taking advantage of the lack of G-R noise over the QD. By first positioning the tip over the QD and then measuring Δf in 20 nm steps until the tip is over the WL (Fig. 2), we find a clear increase in the noise which corresponds to leaving the edge of the QD in just one step as shown in the inset. Thus,

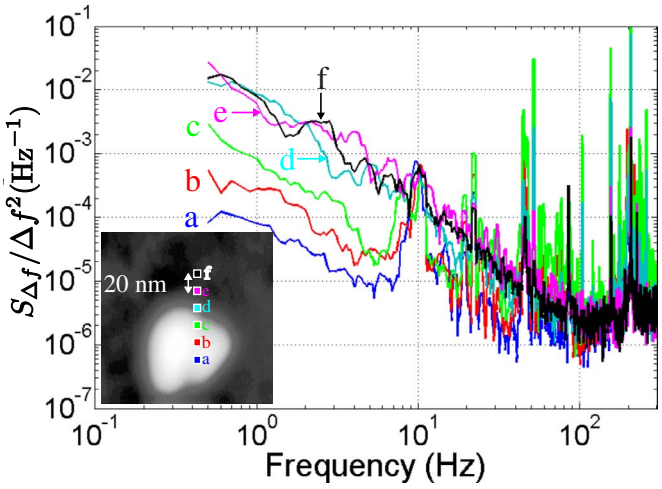

FIG. 2. (Color online) PSD spectra measured at locations indicated by squares with the same color (and letter) shown in the EFM topography image of an InAs quantum dot (inset). Leaving the quantum dot results in the appearance of generation-recombination noise as marked by the approximate −2 slope of the PSD. The data was taken with V_s=2 V at 77 K.

the resolution of this technique is at least 20 nm which is on the order of the tip diameter.

In some sample locations, for small laser intensities and/or small V_s, it becomes possible to detect few fluctuating charge traps resulting in the Δf signal resembling RTN. Figure 3 shows an example of this for V_s=−1 V where three levels are clearly identified. A system with three levels could represent two charge traps with similar potential barriers such that the three possibilities: both empty, both filled, or only one trap empty creates three separate states for the system.

We attribute the observed noise to the following two mechanisms: statistical fluctuations in the number of photoexcited electron-hole pairs and the electron trapping and detrapping in localized defect states. In both cases, electron-hole pairs are created by super-band-gap light illumination but recombine either directly or through recombination centers, respectively. In the first mechanism, generation and recombination of electron-hole pairs occurs over the entire WL

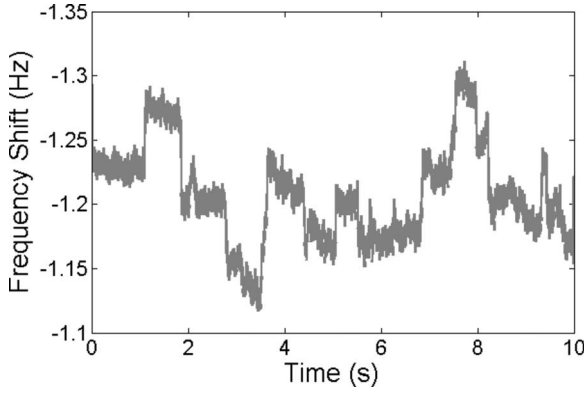

FIG. 3. The Δf measured over the wetting layer at 4.5 K with V_s=−1 V and under laser irradiation. Over this time scale the Δf resembles a multileveled random telegraph signal.

because the process is a band-to-band transition. The fluctuation in the number of electron-hole pairs causes fluctuations in the local band bending, which directly affects the electrostatic force. Generated electron-hole pairs are spatially separated by the built-in electric field leading to a relaxation of the band bending. This process explains the observed streaks which cover the entire WL. The second mechanism is responsible for RTN, as only a few fluctuators are detected when the cantilever tip happens to probe spatially localized trapping centers.

The lack of G-R noise over the QDs can be explained by quantum confinement. The QDs have a confinement energy which is large enough to prevent the separation of charge pairs so that super-band-gap irradiation will not alter the local band-bending on the QD[26,27] and thus no G-R noise is detected with EFM. This observation also convinces us that the noise is not due to the influence of the laser on the cantilever.

The Δf-V_s curves taken with laser off and on [Fig. 4(a)] supports our explanation of the noise. The light irradiation causes two changes in the Δf-V_s curve: a shift in the tip-sample CPD and an increase in the tip-sample force for high positive V_s, both resulting from a change in surface charge. The negative shift of the parabola apex marks the change in CPD due to the change in the surface potential of the sample, while the increased curvature of the parabola belies the increased tip-sample electrostatic force due to the accumulation of charge.[28] The asymmetric response of the noise for high negative [V_s=−5 V, Fig. 4(c)] and positive bias voltages [V_s=3 V, Fig. 4(d)] despite the same magnitude of tip-sample force (marked by similar Δf) indicates that V_s is influencing the charge-pair separation by opposing or complementing (respectively) the built-in electric field within the space-charge layer. All of these observations are consistent with the sample initially having upward band bending due to an excess of negative surface charge trapped in surface states, which is relaxed by the movement of positive charge toward the surface upon the generation of light-induced charge pairs [Fig. 4(b)]. In the presence of the QD, the photoexcited carriers are captured into the QD (via tunneling for electrons and drift for holes) and do not contribute to the reduction in the band bending [Fig. 4(c)].

EFM is capable of spatially locating and characterizing charge traps which significantly affect small-volumed devices. Laser irradiation serves as a means to highlight areas where charge traps reside by providing energy for the traps to become active over shorter time scales. More detailed analysis of the G-R noise or RTN could provide the trapping dynamics of the carriers, which has important implications on the expected behavior of many technically important devices including charge qubits and molecular switches. The trapping dynamics of the photoexcited carriers is of great importance in developing photovoltaic devices. As device size continues to shrink, the spatial resolution of EFM in being able to detect traps will make it instrumental in materials characterization and device development. A particular advantage of EFM over other local electrometry techniques is its high-resolution topography imaging capability which could reveal relationships between structural and noise properties.

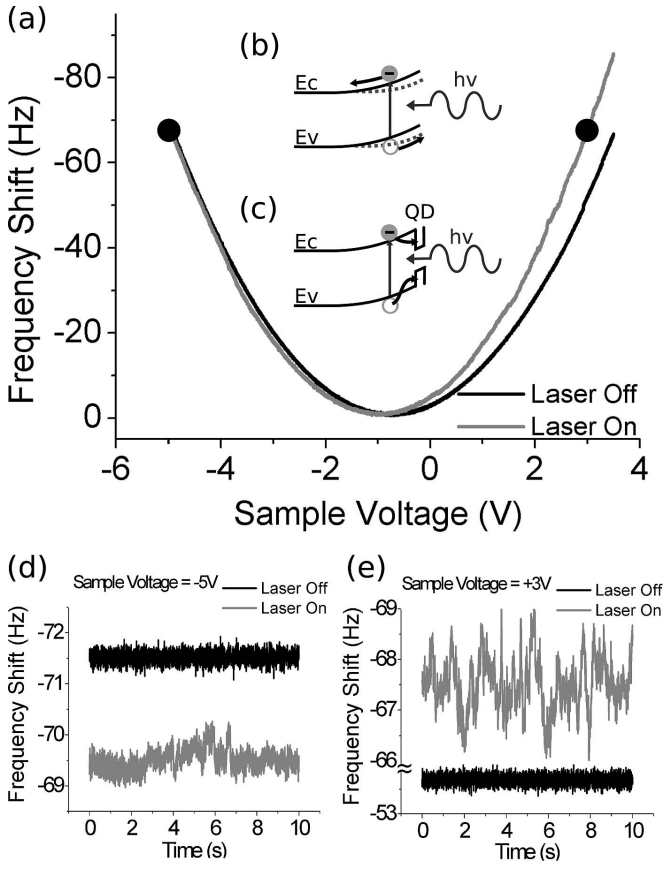

FIG. 4. (a) Δf-V_s curves taken with (gray line) and without (black line) laser irradiation. The laser irradiation causes a negative shift in CPD (parabola apex) and an increased curvature of the Δf-V_s curve. Both observations are a result of a change in surface charge due to the increase in minority carriers which are generated by the light and travel to the surface via electric field, reducing the band bending of the space-charge region near the surface. This effect, which occurs over the wetting layer, is illustrated by the schematic band diagram (b). The effect of the laser on the quantum dot is depicted in (c) where generated charge pairs are captured into the quantum dot and recombine so that an overall charge separation does not occur. Time traces of the Δf for 10 s (d) for V_s=−5 V and (e) for V_s=+3 V are shown. The two time traces under light irradiation (gray line) in (d) and (e) were taken in the conditions indicated by the closed circles (a). More fluctuations are observed at V_s=+3 V than at V_s=−5 V under light irradiation because the applied electric field is complementing rather than opposing the built-in electric field caused by the initial band bending.

The authors would like to thank Philip Poole and Sergei Studenikin at the National Research Council of Canada for providing samples and useful discussion, respectively, and Thomas Szkopek at McGill University for helpful discussions. Funding for this research was provided by the Natural Sciences and Engineering Research Council of Canada, le Fonds Quebecois de le Recherche sur la Nature et les Technologies, and the Canadian Institute for Advanced Research.

*Corresponding author. miyahara@physics.mcgill.ca

[1] J. E. Hill and K. M. Van Vliet, J. Appl. Phys. **29**, 177 (1958).
[2] B. K. Jones, IEEE Trans. Electron Devices **41**, 2188 (1994).
[3] M. J. Deen and F. Pascal, J. Mater. Sci.: Mater. Electron. **17**, 549 (2006).
[4] M. E. Welland and R. H. Koch, Appl. Phys. Lett. **48**, 724 (1986).
[5] E. N. Schulman and R. C. White, Phys. Rev. B **52**, 7864 (1995).
[6] S. Sugita, Y. Mera, and K. Maeda, J. Appl. Phys. **79**, 4166 (1996).
[7] Y. Nakamura, M. Ichikawa, K. Watanabe, and Y. Hatsugai, Appl. Phys. Lett. **90**, 153104 (2007).
[8] M. Field, C. G. Smith, M. Pepper, D. A. Ritchie, J. E. F. Frost, G. A. C. Jones, and D. G. Hasko, Phys. Rev. Lett. **70**, 1311 (1993).
[9] M. J. Yoo, T. A. Fulton, H. F. Hess, R. L. Willett, L. N. Dunkleberger, R. J. Chichester, L. N. Pfeiffer, and K. W. West, Science **276**, 579 (1997).
[10] T. Fujisawa and Y. Hirayama, Appl. Phys. Lett. **77**, 543 (2000).
[11] W. Lu, Z. Ji, L. Pfeiffer, K. W. West, and A. J. Rimberg, Nature (London) **423**, 422 (2003).
[12] R. Schleser, E. Ruh, T. Ihn, K. Ensslin, D. C. Driscoll, and A. C. Gossard, Appl. Phys. Lett. **85**, 2005 (2004).
[13] M. Pioro-Ladriere, J. H. Davies, A. R. Long, A. S. Sachrajda, L. Gaudreau, P. Zawadzki, J. Lapointe, J. Gupta, Z. Wasilewski, and S. Studenikin, Phys. Rev. B **72**, 115331 (2005).
[14] E. Vidal Russell and N. E. Israeloff, Nature (London) **408**, 695 (2000).
[15] Y. Kawano and T. Okamoto, Appl. Phys. Lett. **87**, 252108 (2005).
[16] C. Schonenberger and S. F. Alvarado, Phys. Rev. Lett. **65**, 3162 (1990).
[17] E. Bussmann and C. C. Williams, Appl. Phys. Lett. **88**, 263108 (2006).
[18] R. Stomp, Y. Miyahara, S. Schaer, Q. Sun, H. Guo, P. Grutter, S. Studenikin, P. Poole, and A. Sachrajda, Phys. Rev. Lett. **94**, 056802 (2005).
[19] M. Vogel, B. Stein, H. Pettersson, and K. Karrai, Appl. Phys. Lett. **78**, 2592 (2001).
[20] P. J. Poole, J. McCaffrey, R. L. Williams, J. Lefebvre, and D. Chitrani, J. Vac. Sci. Technol. B **19**, 1467 (2001).
[21] M. Roseman and P. Grutter, Rev. Sci. Instrum. **71**, 3782 (2000).
[22] Type NCLR: Nanosensors http://www.nanosensors.com
[23] D. Rugar, H. J. Mamin, and P. Guethner, Appl. Phys. Lett. **55**, 2588 (1989).
[24] T. R. Albrecht, P. Grutter, D. Horne, and D. Rugar, J. Appl. Phys. **69**, 668 (1991).
[25] The PSD was calculated by fast Fourier transform using a Hamming window.
[26] G. Dumitras, H. Riechert, H. Porteanu, and F. Koch, Phys. Rev. B **66**, 205324 (2002).
[27] C. H. Chan, Y. S. Huang, J. S. Wang, and K. K. Tiong, Opt. Express **15**, 1898 (2007).
[28] D. C. Coffey and D. S. Ginger, Nature Mater. **5**, 735 (2006).